High Ionic Strength and Low pH Detain Activated Skinned Rabbit Skeletal Muscle Crossbridges in a Low Force State

CHUN Y. SEOW and LINCOLN E. FORD

From the Cardiology Section, Department of Medicine, The University of Chicago, Chicago, Illinois 60637

ABSTRACT The effects of varying pH and ionic strength on the force–velocity relations and tension transients of skinned rabbit skeletal muscle were studied at 1–2°C. Both decreasing pH from 7.35 to 6.35 and raising ionic strength from 125 to 360 mM reduced isometric force by about half and decreased sarcomere stiffness by about one-fourth, so that the stiffness/force ratio was increased by half. Lowering pH also decreased maximum shortening velocity by ~29%, while increasing ionic strength had little effect on velocity. These effects on velocity were correlated with asymmetrical effects on stiffness. The increase in the stiffness/force ratio with both interventions was manifest as a greater relative force change associated with a sarcomere length step. This force difference persisted for a variable time after the step. At the high ionic strength the force difference was long-lasting after stretches but relaxed quickly after releases, suggesting that the structures responsible would not impose much resistance to steady-state shortening. The opposite was found in the low pH experiments. The force difference relaxed quickly after stretches but persisted for a long time after releases. Furthermore, this force difference reached a constant value of ~8% of isometric force with intermediate sizes of release, and was not increased with larger releases. This value was almost identical to the value of an internal load that would be sufficient to account for the reduction in maximum velocity seen at the low pH. The results are interpreted as showing that both low pH and high ionic strength inhibit the movement of crossbridges into the force-generating parts of their cycle after they have attached to the actin filaments, with very few other effects on the cycle. The two interventions are different, however, in that detained bridges can be detached readily by shortening when the detention is caused by high ionic strength but not when it is caused by low pH.

INTRODUCTION

It is generally believed that force and shortening of muscle are generated by the cyclical attachment and detachment of myosin crossbridges to actin thin filaments (Huxley, 1957) with a force-producing power stroke occurring during the attachment phase of the cycle (Huxley and Simmons, 1971). It is further known that there are

multiple chemical and mechanical transitions in the complete cycle, and there is a close coupling between these two types of transitions (see reviews by Taylor, 1992 and Huxley, 1980). One proposal to account for this coupling is that the chemical reactions (substrate binding, hydrolysis, product release) alternate with the mechanical transitions (crossbridge attachment, power stroke, crossbridge detachment) (Huxley, 1980). Such proposals suggest that substantial insight into the energy transduction process in muscle might be gained from a knowledge of the sequence of these transitions. Thus, we have undertaken a series of studies on the effects of chemical environment on the mechanical transitions in the crossbridge cycle with the intent of learning more about the exact sequence of reactions. Since it is well known that changes of ionic strength (Thames, Teichholz, and Podolsky, 1974; Julian and Moss, 1981) and pH (Edman and Mattiazzi, 1981; Metzger and Moss, 1987; Chase and Kushmerick, 1988; Cooke, Franks, Luciani, and Pate, 1988) strongly influence the steady-state contractile properties of muscle, we have begun this series with a study of the effects of these ionic changes on the crossbridge cycle. In addition to providing information about the crossbridge cycle, these experiments provide necessary information about the range of variation that might be encountered from changes of pH and ionic strength. Because most of the transitions in the cycle are likely to result from the making and breaking of ionic bonds among the contractile proteins, it might be expected that chemical alterations that influence protein ionization would strongly influence the crossbridge cycle. The results suggest the opposite, however; all of the effects of changing pH and ionic strength can be accounted for by changes in the initial transitions associated with crossbridge attachment, with very little effect detected elsewhere in the cycle.

METHODS

Force–velocity characteristics and tension transients were studied in skinned rabbit psoas fibers near zero degrees. Low temperature was used to slow the responses for more accurate measurement and to diminish the developed force so as to minimize fiber deterioration. For force–velocity experiments, velocity was measured early in the steady state "phase 4" (Huxley and Simmons, 1973) of isotonic shortening, as previously described (Seow and Ford, 1991, 1992). Tension transients were measured as the force responses to rapid changes of sarcomere length. Sarcomere length was measured and servo controlled using a laser diffraction system. Paired observations were always made in the same fiber, and the results were expressed initially as the relative differences between the control and test observations. Where appropriate, these results have been converted to absolute dimensions using the average values for the control observations.

The rabbit fast muscle preparation described previously (Seow and Ford, 1991, 1992) was used except that most of the fibers were obtained from muscles within 1–3 d after the animal was killed. Frequently, the muscle were not glycerinated but simply skinned by soaking overnight in a solution of low divalent cation and stored at 0°C before use.

Solutions

Solution composition was planned to yield desired ionic strengths and compositions using a computer program kindly given to us by Dr. R. E. Godt. All experimental solutions contained 5 mM MgATP, 1 mM free Mg^{2+}, 20 mM creatine phosphate, 10 mM imidazole, 56 g/liter dextran T-70, and sufficient K-propionate to yield the desired ionic strength. The pH of each

solution was adjusted to the desired value at 1–2°C. Relaxing solution contained 5 mM EGTA. Contracting solution contained calcium buffered to pCa 4.8 with 5 mM EGTA. A rinse solution containing 0.1 mM EGTA was used to lower the EGTA concentration immediately before each activation.

In experiments where ionic strength was varied, two stock solutions of the extreme values of ionic strength (125 and 600 mM) were mixed together to obtain the desired value. In experiments where pH was varied, the pH of the individual solutions was adjusted at 2°C using KOH or propionic acid after an initial adjustment with K-propionate to account for the differences in ionic composition.

The glycerol storage solution was made by mixing equal quantities of glycerol and relaxing solution without Dextran T-70. The skinning solution had the composition of relaxing solution except that Dextran T-70 was omitted and the total $MgCl_2$ concentration was 1 mM in the presence of 5 mM ATP, so that the concentration of free divalent cations was very low.

Apparatus

Most of the apparatus has been described previously. Briefly, the fibers were held horizontally in a trough into which precooled solutions could be injected (Chiu, Quinlan, and Ford, 1985). Overall muscle length was servo controlled by a linear actuator-type moving coil servo motor connected to one end of the fiber. The other end was attached to the vertical arm of a piezoelectric force transducer (Chiu, Karwash, and Ford, 1978) adjusted to have a resonant frequency of 10 kHz. Sarcomere length was sensed from the position of the first diffracted order of a 10-mW helium-neon laser beam passing through the fiber (Seow and Ford, 1992). A set of cylindrical and spherical lenses shaped the beam into a narrow slit of approximately uniform intensity that was focused on the entire length of the fiber and then focused to a point on a linear position-sensing detector (LSC/5d; United Detector Technology, Hawthorne, CA). The output of the position detector was proportional to both the position and intensity of the first diffracted order. To compensate for variations in the intensity of the first order, the output of the position detector was divided by a signal proportional to the intensity of light reaching the detector. In addition to light in the first order, this denominator signal also included background light. Partial compensation for this background light was made by placing photodiodes at either end of the linear detector and subtracting their average output from the denominator signal. An electronic analogue shaping network was used to convert the position of the first order to a signal proportional to sarcomere length over the range of 2.3–2.5 μm (Goldman and Simmons, 1984). The sarcomere length sensor was calibrated initially by two physical means. First, the fourth diffracted order from a 10-μm grating was used to obtain a spot of light at a position corresponding to 2.5 μm sarcomere spacing. The gain and offset of the linear detector were then adjusted so that the output from this stage was +5 V when the diode was in the normal position and −5 V when it was reversed. This calibration was compared with a second method in which the position of a spot of light could be made to vary precisely. The apparatus was adjusted until the two methods agreed. This physical calibration was compared with a functional calibration, described below, at the beginning of every activation used for tension transients. Data were included only when these functional calibrations met specific criteria.

Data were recorded and the experiments controlled using an IBM-compatible computer equipped with a Tekmar Co. (Cincinnati, OH) Labmaster interface board programmed by SALT software (Fenster and Ford, 1985; Wirth and Ford, 1986).

Protocols

Fiber segments were activated continuously throughout a set of steps under a single condition. The Brenner protocol (Brenner, 1983; Sweeney, Corteselli, and Kushmerick, 1987) of repeti-

tively shortening the fibers at or near their maximum velocity and rapidly restretching them to their starting length was used to maintain sarcomere homogeneity. After the fiber was first activated, and before a set of steps was begun, an analogue ramp generator was used to impose 300-ms ramps every 2.5 s. When recordings were to be made, the computer sensed the onset of the ramps and imposed tension or length steps on the same schedule. Both sarcomere length steps and isotonic releases were followed by a rapid release sufficiently large to make the fibers go slack for at least 80 ms, after which the fibers were restretched to their starting length. These large steps were used both to zero the force transducer and to allow the fibers a sufficient period of unloaded shortening to maintain good sarcomere patterns. Both types of steps were made in groups of nine, ~2.5 s apart, and then the fibers were relaxed. The force–velocity studies used methods that have been described previously (Seow and Ford, 1991, 1992); the tension transient experiments are described here.

Tension Transients

With both types of studies, the fibers were activated continuously during a set of nine steps, and control and test activations were alternated. One additional procedure was added to calibrate the sarcomere length sensor in each activation period. After the fiber was activated and before the set of nine steps, a single step to an isotonic load of ~20% of isometric force was made. Changes in overall muscle length and sarcomere length were measured over the interval from 50 to 142 ms of isotonic shortening. The change in overall muscle length was divided by the numbers of half-sarcomeres to estimate shortening in units of nanometers per half-sarcomere. The change in sarcomere length was then divided by this value to obtain the "S/L ratio." The data were not used unless two criteria were met. The first was that the S/L ratio for any activation fall within the range of 0.9–1.1. The second was that the absolute difference between the S/L ratios obtained under control and test conditions not differ by >2%. Sarcomere length changes were always assessed from the sarcomere length records after the length change had been divided by the S/L ratio.

After the calibration was assessed, the fibers were placed in S control and nine sarcomere length steps were applied. The S steps proceeded from the largest stretch, ~2 nm/half-sarcomere, to the largest release, ~10 nm/half-sarcomere. The step size was adjusted so that the sixth step in the series (the fourth release) would cause force to fall near zero under the activating conditions that produced the greatest relative stiffness. Step size increments were adjusted to be one-fourth of this value. The incremental change in step size was the same for these first six steps. For the next three, the incremental increase was twice as great. For the first six steps, the steps were made as rapidly as the servo system would allow (~250 μs in S control). With the three subsequent releases, however, this speed of step would drive the fiber to go slack, so that servo control of sarcomere length could not be maintained. To avoid this potentially damaging situation, the step speed was slowed for the last three steps: the seventh and eighth steps took ~2 ms to complete and the ninth ~4 ms. These last three steps were used mainly for determining T_2 levels.

The recording speed was not constant during the sarcomere length steps. During the isometric period before the step and the slack period at the end of the record, the digital sampling interval was 0.8 ms per conversion of each signal. The isometric period lasted 20 ms and the slack period 30 ms. 188 points were recorded between the isometric and slack periods, but the data conversion period was changed several times. For 1.8 ms during and immediately after the steps, the records were sampled at 60-μs intervals (30 samples), and for the next 2.4 ms (20 more samples) the recording interval was lengthened to 120 μs. The next 100 samples were converted at 2-ms intervals in stretches and 1-ms intervals in releases. The final 38 samples before the slack release were converted at 5-ms intervals. Longer recordings were made after stretches because the transient responses associated with stretches were slower.

If the L/S ratios for pairs of control and test activations met the criteria described above, the individual steps were assessed for quality and speed of step and for the absence of noise (see below). If more than one pair of steps of a given size met all the criteria for inclusion, the individual records for each type of activation, control or test, were signal averaged and treated as a single record. If only one pair of records for a given step size met all the criteria for inclusion, it also was included as a single record for that fiber. These individual single records for each fiber, for each step size, and for each type of activation were then signal averaged to provide a final set of records.

One of the major results to be obtained from these records is the difference between averaged control and test force records. These difference records were obtained by subtracting a shifted, and sometimes scaled, control record from a test record. In general, measurements were made from these signal-averaged records. An exception is the measurement of T_1, the extreme tension change associated with the step, as described below.

Exclusion of Data

As previously described, there was a moderate amount of scatter in velocities measured at very low isotonic loads, below ~ 0.01 mN (Seow and Ford, 1991, 1992). For this reason, force–velocity data were not included for loads below this level. No other force–velocity points were excluded. In transient experiments there were several criteria for inclusion. As described above, records from pairs of activations were included if the S/L ratios for the control and test activation did not differ by $>2\%$ and if both S/L ratios fell within the range of 0.9–1.1. In addition, the quality of each record was evaluated separately, and pairs of records were excluded if the records were noisy or if the steps were slowed. In spite of these more rigid criteria, at least one pair of records for each step size from each fiber was included for signal averaging. This completeness was achieved because in most fibers several pairs of activations meeting the S/L ratio were included, so that at least one record for each step size was available.

Control Observations

Measurement of T_1. It was consistently found that the mean values of the extreme tension deviations were greater by a few percent when the measurements were taken as the average of the individual records, as compared with the single measurements made from the signal-averaged record. This difference is shown in Table I. For each size of step the sarcomere compliance was determined both from the average of the individual records (method A) and from direct measurement of the signal averaged record (method B). The sarcomere compliance is expressed as the amount of sarcomere shortening (y_0) that would be required to bring isometric force to zero if this compliance were correctly determined from the step. In every case, method A yields slightly lower compliance, and the disparity would be expected if the extreme tension (T_1) were reached at slightly different times in different records; the T_1 level of the averaged record would not be as extreme as the average of the individual extremes. For these measurements, therefore, the extreme tension change and sarcomere length change were measured individually and averaged.

Series elastic elements. When sarcomere length steps were applied, additional length changes had to be made to the overall muscle length to compensate for changes in series elastic element extension. These differences are illustrated in Fig. 1, where the sarcomere length and overall muscle length records have been superimposed for four sizes of step. The overall muscle length change has been divided by the number of half-sarcomeres between the clips, so that this length change could be compared in the same units with the sarcomere length changes. As expected, the difference between the two types of length change is greatest at the end of the step, when the force change was greatest, and the difference decreased with time as the force

TABLE I

Relative Sarcomere Compliance ($y_0[nm/P_0]$) Obtained from Different Step Sizes and Methods of Averaging

Step	Ionic strength 360 mM			Ionic strength 125 mM			pH 6.35			pH 7.35		
	A	B	A/B	A	B	A/B	A	B	A/B	A	B	A/B
1	2.17	2.27	0.956	3.20	3.31	0.967	1.94	2.00	0.970	3.03	3.14	0.965
2	2.22	2.24	0.991	3.16	3.38	0.935	2.03	2.04	0.995	3.02	3.09	0.977
3	2.85	2.95	0.966	3.60	3.76	0.957	2.33	2.36	0.987	3.51	3.60	0.975
4	2.90	2.95	0.983	3.92	3.95	0.992	2.51	2.66	0.944	3.63	3.68	0.986
5	3.23	3.29	0.982	4.09	4.22	0.969	2.70	2.78	0.971	3.87	3.89	0.995
6	3.74	3.76	0.995	4.47	4.50	0.993	3.06	3.13	0.978	4.11	4.25	0.967

Relative sarcomere compliance (y_0) is expressed as half-sarcomere shortening that would be required to bring force from its isometric value (P_0) to zero, if sarcomere stiffness were represented by a line passing through the isometric point and T_1 point. In method A, compliance was determined from the average T_1 of the individual records; in method B, compliance was determined from the final, signal averaged record.
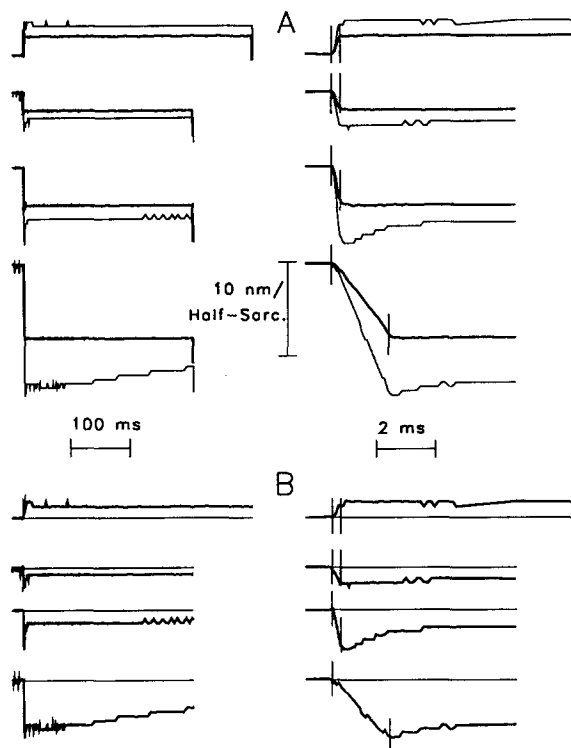

FIGURE 1. Superimposed sarcomere length (*thicker lines*) and overall muscle length (*thinner lines*) records for four sizes of step (*A*). The overall muscle length change has been divided by the number of half-sarcomeres to compare the two types of length changes in the same dimensions. Step size was chosen so that the third step would just bring force to zero. The second step was a release of half this size and the first step a stretch of the same size as the small release. The stretch was maintained for a longer time because the force responses to stretches were slower. The fourth step was a release about twice the size of the third step, and was slowed to avoid making the muscle go slack. Large shortening steps were applied at the end of the recording period to make the force go slack,

so as to zero the force transducer. The early portions of the same records are shown at a 50 times faster speed in the right-hand panels to resolve the events associated with the steps. The vertical cursors on these high speed records indicate the time of the beginning of the step and the time of the extreme tension change (T_1). (*B*) The difference between the two types of record. The differences at the end of the steps and at the ends of the record are plotted in Fig. 2. Ionic strength 125 mM; pH 7.0.

recovered, but the decrease was much less than would have been expected from an undamped compliance. Thus, for a given force change, there was a substantially greater difference in the length records at the end of several hundred milliseconds than there was at the end of the step. This difference is shown in Fig. 2, where the instantaneous force is plotted against the difference in length change both at the end of the step and the end of the recording period. The slopes of these two curves differ by a factor of four. The explanation is that only about one-fourth of the total series compliance can be considered undamped on the time scale of the applied steps. These plots also indicate that the compliance in series with the sarcomeres was quite stiff; 0.4% muscle length shortening of the undamped series elastic element was required to bring force to zero from its isometric value.

Preservation of fiber function. Some previous studies of skinned muscle have reported a progressive deterioration of function, as measured by a decline in isometric force with each successive activation (see, for example, Podolin and Ford, 1986). In the present experiments there was almost no such decline of force, even though the fibers were activated for much longer periods. Of note is that no decline of isometric force was seen even when the fibers were
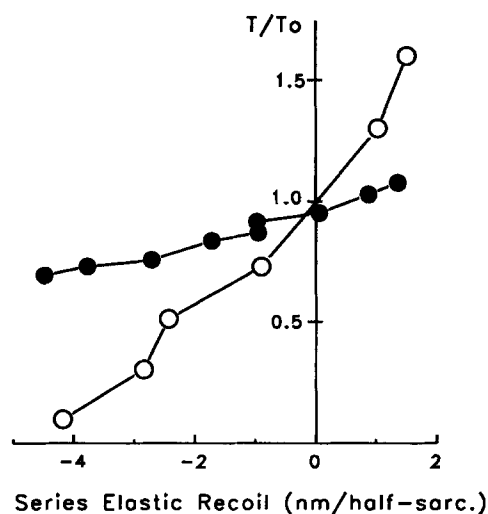

FIGURE 2. Series elastic element recoil, determined as the difference between sarcomere length change and overall muscle length change at the end of the step (*open symbols*) and at the end of the record (*filled symbols*). The length difference is plotted as abscissa and the relative force at the time of the measurement as ordinate. Length differences at the end of the step are not plotted for releases larger than 4 nm/half-sarcomere because these steps were slowed. The large difference between the two curves is attributed to damped recoil of structures in series with the sarcomeres.

activated several times at an ionic strength of 600 mM. We had expected that this high ionic strength would dissolve the myosin thick filaments. The lack of dissolution might be due to the brief exposures, usually less than a minute for each activation, or to the fibers having been activated, and therefore held in a more rigid lattice, for most of the period of exposure. We attribute the generally better preservation of function to the use of the Brenner (1983) protocol for maintaining sarcomere homogeneity.

RESULTS

Force–Velocity Relations

Force–velocity measurements were first made in exploratory experiments to determine the best conditions for comparing tension transient responses. Data were collected in paired experiments and the values obtained under test conditions were expressed as fractions of those obtained in control experiments (Fig. 3, *A* and *B*).

The absolute values obtained under the control conditions are listed in Table II. As shown in Fig. 3 A, increasing ionic strength decreased isometric force with very little change in velocity at all relative loads. Over the range of ionic strength studied, isometric force fell threefold, while the maximum ranges of variation in maximum velocity and relative maximum power were 12 and 17%, respectively. The slight decrease in relative maximum power with a slight increase in maximum velocity indicates that the force–velocity curves became slightly more curved at high ionic strength. By contrast, Fig. 3 B shows that lowering pH decreased both isometric force and maximum velocity. At pH 6.35 isometric force and maximum velocity were 58
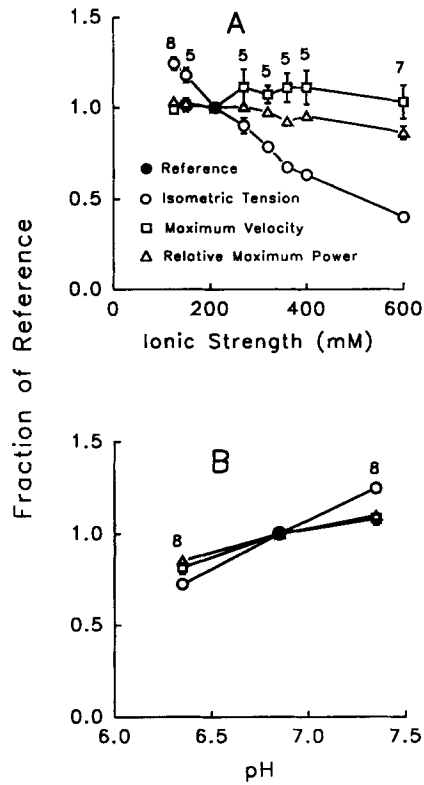

FIGURE 3. Changes in isometric force, maximum velocity, and relative maximum power as functions of ionic strength (A) and pH (B). Numbers above the symbols indicate the number of fibers averaged.

and 75%, respectively, of their values at pH 7.35. The nearly identical changes in maximum velocity and relative maximum power indicate very similar curvature of the force–velocity curves at the different pH's.

On the basis of the data in Fig. 3, A and B, the conditions chosen for investigation in the transient experiments were pH 6.35 compared as the test with pH 7.35 used as control and 360 mM ionic strength compared as test with 125 mM as control. There was an approximate twofold reduction in isometric force in each of the test conditions compared with their respective controls. The ionic strength for the pH experiments was 210 mM and the pH in the ionic strength experiments was 7.0.

In addition to the force–velocity data presented in Fig. 3, which were obtained in an initial set of experiments, most of the fibers used to study tension transients were also studied in isotonic experiments to obtain a separate set of force–velocity comparisons. The ratios of test to control parameters obtained from these separate experiments are compared with the same conditions in the original set in Fig. 4. As indicated, the changes in the force–velocity data obtained with the two populations of fibers are nearly identical.

Internal Load

The absence of a substantial change in maximum velocity or relative maximum power with increased ionic strength might suggest that this intervention only served to diminish the number of active cross-bridges, in much the same way as a decrease in activation might do (Ford, 1991). The substantial change in velocity seen with decreased pH requires an additional factor. A possible factor, considered here, is an increased internal load. When such an internal load exists, the contractile elements

TABLE II

Control Values of Isometric Tension, Maximum Velocity, and Relative Maximum Power

	P_0	V_{max}	PV_{max}	No. of fibers
	mN	$\mu m \cdot h - s^{-1} \cdot s^{-1}$	$\mu m \cdot h - s^{-1} \cdot s^{-1}$	
Ionic strength 125 mM (pH 7.0)	0.566 ± 0.082	0.623 ± 0.043	0.054 ± 0.002	8
Ionic strength 210 mM (pH 7.35)	0.460 ± 0.028	0.690 ± 0.015	0.047 ± 0.002	7

Means and standard errors are listed. Both V_{max} and PV_{max} are expressed in units of micrometers per half-sarcomere per second.

cannot be fully unloaded, and their true maximum velocity cannot be achieved. Such a load should not alter the true force–velocity relations of the contractile elements; it merely diminishes the measured external force so that the force–velocity curves are only truncated, but not altered in shape. As a consequence, the velocity asymptote b in the Hill (1938) equation should not be altered. Thus, the first test of the presence of an internal load is that the value of b is unchanged. (For a detailed explanation, see Ford and Forman, 1974 and Ford, 1991). In the final set of pH experiments the mean values of b were nearly identical, 0.128 and 0.114, respectively, at pH 6.35 and 7.35, indicating that all the changes in the curves could be accounted for by an internal load. This load can be calculated from the increase in the ratio of the force asymptote a to the isometric force, as follows.

When the values of b are the same, the curves relating the velocity to the total force on the contractile elements, the total force plus the internal load, can be made to superimpose by scaling the curves to the total load. Thus, the ratios of the force asymptote a to isometric force P_0 will be identical when both a and P_0 are corrected

for the internal load L. Expressed algebraically:

$$(a/P_0)_c = \frac{(a_t - L)}{(P_{0_t} + L)} \tag{1}$$

where the subscripts c and t indicate the control and test values, respectively. Solving for the value of L yields:

$$L = \frac{[(a/P_0)_t - (a/P_0)_c]}{[1 + (a/P_0)_c]} \cdot (P_0)_t \tag{2}$$

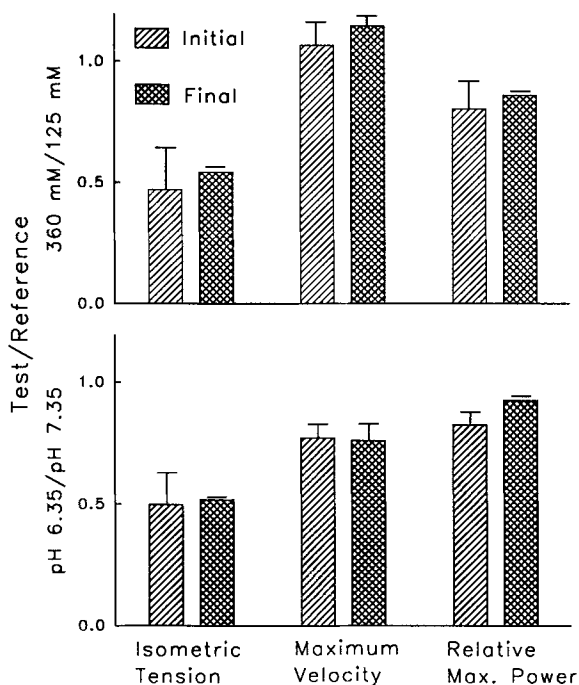The values of a/P_0 were 0.261 and 0.165 at pH 6.35 and 7.35, respectively.

FIGURE 4. Ratio of test to control parameters of the force–velocity curves in an initial series, used to define only the force–velocity relations, and a final series of fibers also used for tension transient experiments. Error bars indicate SEM. The errors of these percentages are generally larger in the initial set because the two conditions were not compared directly in the same fibers, as they were in the final series. There were seven fibers in the final pH series and eight in the final ionic strength series. The numbers of fibers in the initial series are indicated in Fig. 3.

Substituting these values into Eq. 2 indicates that an internal load equivalent to 8% of the isometric force at the lower pH could account for all the observed decrease in maximum velocity. This value is used in analyzing the transient responses below.

Tension Transients

A set of nine sarcomere length steps, two stretches and seven releases, was used to define the tension transient responses under each condition. The results from a group of fibers treated identically were signal averaged to obtain a final set of records. 8 fibers were averaged in the pH experiments and 11 fibers in the ionic strength experiments. The final result of these experiments is a comparison of the control and test signal-averaged records for each step size. Before presenting these

comparisons, the transients obtained under control conditions in the ionic strength experiments will be described.

Control records. The signal-averaged force records for the nine sizes of step are shown at two recording speeds in Fig. 5. These records show the four characteristic phases originally described by Huxley and Simmons (1971, 1972). The extreme tension reached (T_1) during the step (in phase 1) and the tension approached (T_2) during the rapid, early force recovery (phase 2) are plotted as a function of step size
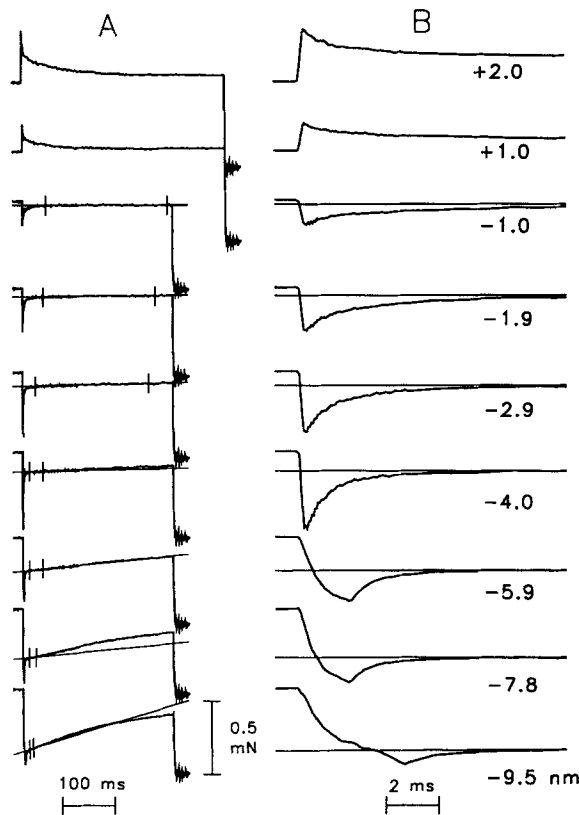

FIGURE 5. Tension transients obtained under the control conditions in the ionic strength experiments (125 mM). The same records are shown at a 50 times faster speed on the right (B) than on the left (A). The size of the sarcomere length change is printed next to each high speed record. A line was fitted through the pause or inflection in force recovery (phase 3) over the interval indicated by the cursors on each of the slow release records. No lines were fitted to the stretch records because no inflections were found. The value of this line at the time of the midpoint of the sarcomere length step (T_2) is plotted against step size in Fig. 6, as is the value of the extreme tension reached (T_1). The early, rapid (phase 2) force recovery was isolated by subtracting the force record from the line over an interval from the time of the extreme tension change to the time that the record reached the line. These isolated rapid force recoveries are plotted in Fig. 7.

in Fig. 6. The T_2 levels were determined by fitting lines to the records during the pause or inflection in tension recovery (phase 3) and extrapolating these lines to the time of the midpoint of the step (Ford, Huxley, and Simmons, 1977). These lines are drawn on all the release records in Fig. 5. No such lines are drawn on the stretch records because no pauses or inflections were seen after stretches. As a consequence, no T_2 values were determined for stretches. The T_1 and T_2 curves for this preparation

(Fig. 6) look very similar to those described by Ford et al. (1977) for frog muscle at 0°C except that the T_1 curves are substantially steeper.

As with frog muscle, the speed of the rapid partial recovery of force during phase 2 was slowest with stretches and fastest with large releases. To quantify this change in speed, the rapid recovery was isolated by subtracting the early force values from the line fitted through phase 3. These isolated recoveries are plotted in Fig. 7 A. The amplitude of this rapid force recovery was then scaled by dividing the force at each instant by the extreme tension change that would have occurred if the T_1 value were an extrapolation of the T_1 level achieved in the largest stretch (Fig. 7 B). This normalization procedure plots the early force recovery as a fraction of its greatest value, and corrects for the greater degree of truncation of force that occurs with the faster phase 2 recoveries in larger releases. The increased speed of recovery in large releases is obvious from these scaled records. The records are not exponential and cannot be described by a time constant, but they can be made to superimpose quite closely if the time from the midpoint of the step in each record is scaled by a constant
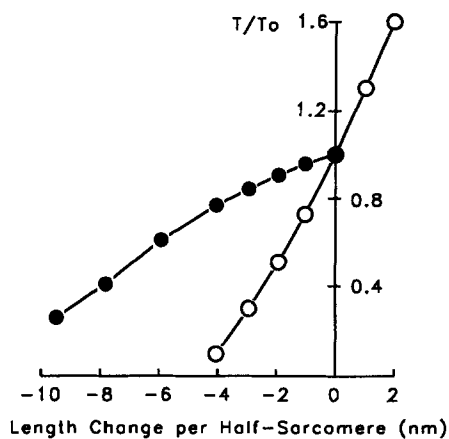

FIGURE 6. T_1 (open symbols) and T_2 (filled symbols) curves for the ionic strength control experiments.

(Fig. 7 C). The time scaling constant for each step, as represented by the initial half-time for each record, is plotted as function of step size in Fig. 8. These time scaling factors vary ~ 10-fold, in a manner that is very similar to frog muscle (Ford et al., 1977).

It will not be necessary to describe in great detail the transients obtained at higher ionic strength and lower pH because the experimental records differ from the controls in only a few very specific ways.

Effects of altered pH and ionic strength. To show the effects of the test conditions, the test records were scaled to the controls so that their isometric forces coincided and then superimposed. Such scaled and superimposed records for three sizes of step comparing high and low ionic strength are shown in Fig. 9 A. The high ionic strength (test = 360 mM) is plotted as the thick trace and the lower ionic strength (control = 125 mM) is plotted as the thin trace. The difference records (control minus scaled test) for all nine steps are plotted in Fig. 9 B. For stretches, the scaled test records deviate above the control records during the step, and the difference

achieved at the end of the step decays very slowly over the entire period of recording. For releases, the scaled records do not deviate as much as for comparably sized releases, and the differences decay within a few milliseconds after the end of the step. It should be noted that the speed of the decay increases with increasing size of release.
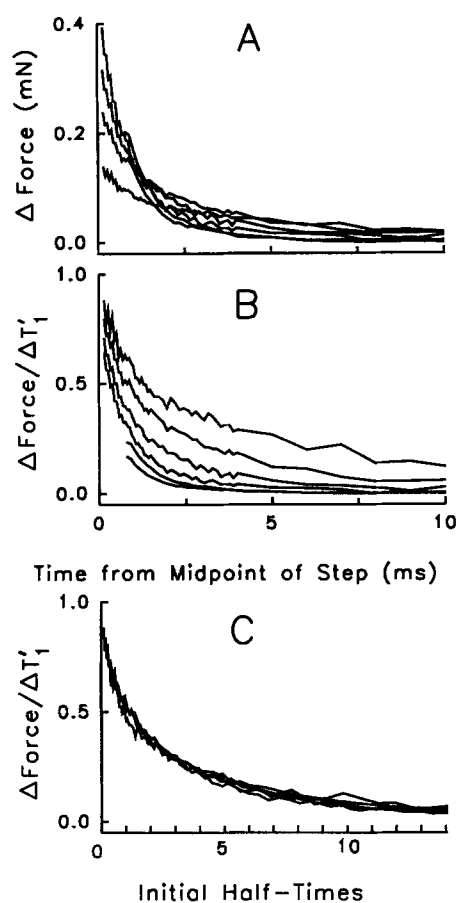

FIGURE 7. Isolated phase 2 force recovery in releases. Time is taken from the midpoint of the sarcomere length step. The largest release has been omitted because most of the record had been truncated by the rapid force recovery and the slowed step speed. (A) The unscaled records are difficult to follow because all of the records cross each other. (B) The amplitudes of the records have been scaled to represent force as a fraction of the value (T'_1) that would have been achieved if the T_1 level at the end of the step were a direct extrapolation of the T_1 level in the largest stretch. The individual records are more easily identified because the individual records do not cross and the records progress from the smallest step at the top to the largest step at the bottom. This ordering occurs both because the recoveries are progressively more rapid in the larger steps and because the amplitude of the observed response varies in inverse proportion to the step size, as more of the force change is truncated by rapid recovery during the step. (C) The time axis for each record has been scaled to make the records superimpose as closely as possible. Time is plotted in increments of the time taken for normalized force to fall to half. The time scaling factor is plotted as a function of step size in Fig. 8.

A similar set of records comparing the effects of pH 6.35 with pH 7.35 is shown in Fig. 10. The effects of lowering pH were similar to raising ionic strength except that the effect of step direction was reversed. The scaled test records deviated from the controls during the steps, and the difference between test and control records declined to zero very rapidly after stretches but decayed only partially after releases.
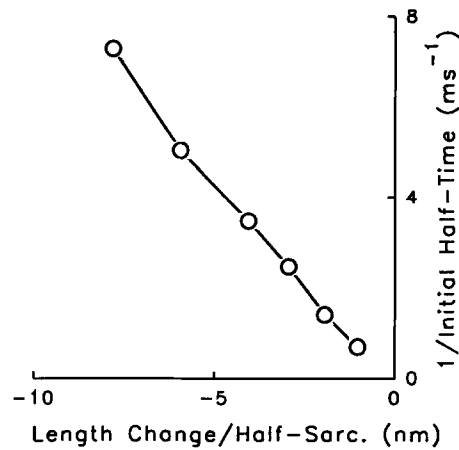
FIGURE 8. Time taken for the scaled forces in Fig. 7 to fall to half. The plot also indicates the relative value of the scaling factor used to make the scaled records superimpose.

The decay after release also progresses in two distinct phases. The first is a very rapid decay whose speed and dependence on step size is similar to that seen in high ionic strength. The second is a much slower decay to a level that appears to be nearly constant over the recording interval used here. As with the more rapid decay, the speed of this process is increased with larger sizes of release. The residual tension
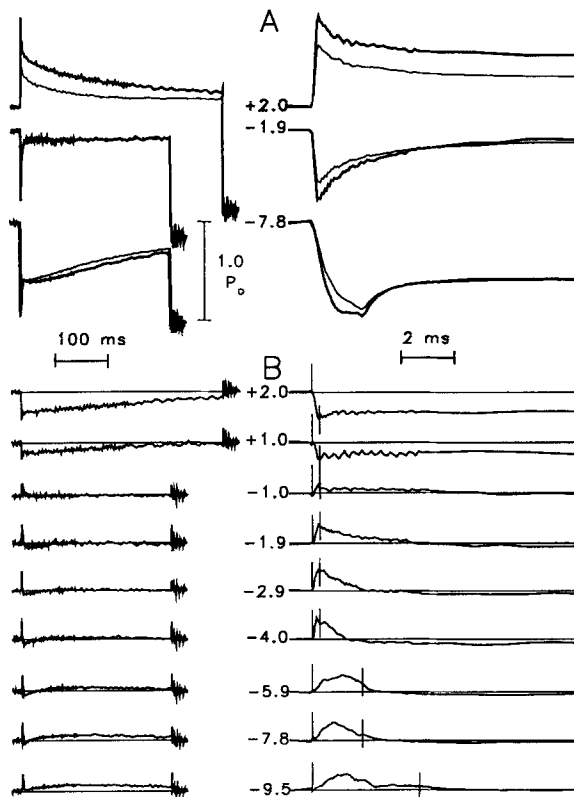

FIGURE 9. Effect of ionic strength on the tension transients. (A) Force responses obtained at two ionic strengths (125 and 360 mM) superimposed for three sizes of step. The amplitudes of the records have been scaled so that their isometric forces coincide. The same records are shown at a 50 times greater speed in the right-hand panels. The thinner traces were obtained at 125 mM ionic strength (control) and the thick records at 360 mM (test). (B) The difference records (control minus test) for all nine step sizes. Step size, in nanometers per half-sarcomere, is printed next to each record. Vertical cursors on fast records indicate the time of onset of step and time of maximum tension deviation (T_1). Responses from 11 fibers have been signal averaged for each pair of records.
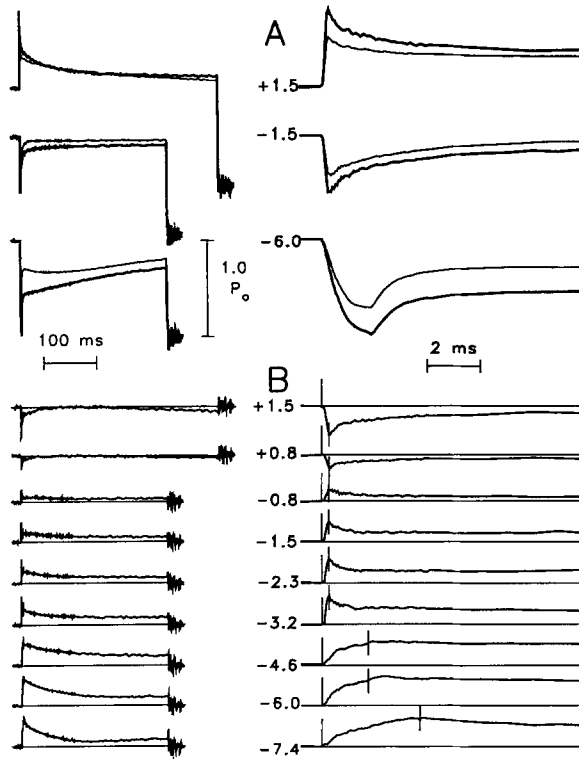
FIGURE 10. Effect of pH change on the tension transients. As in Fig. 9, but with the control (thin) traces obtained at pH 7.35 and the test (thick) traces obtained at pH 6.35. Responses of eight fibers have been signal averaged for each pair.

difference at the end of the recording period is plotted as a function of step size in Fig. 11. As shown, this residual tension increases with small releases to reach a constant value of ~8–10% of the isometric force at a step size of ~5 nm/half-sarcomere. The amount of internal load that would be required to explain the changes in the force–velocity curves at low pH is plotted as the interrupted horizontal line in Fig. 11. As shown, there is good agreement between this calculated internal load and the steady residual force difference seen after large releases at low pH.

Changes in stiffness and compliance. The T_1 levels, reflecting the instantaneous stiffness of the muscles under the different conditions, are plotted as a function of
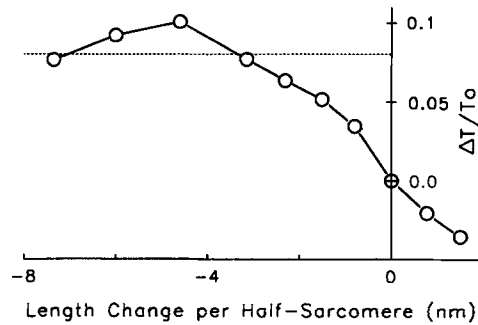

FIGURE 11. Tension difference at the end of the recording period in the pH experiments. This difference achieves a nearly steady value with larger releases. The value of internal load required to produce the decrease in maximum velocity at low pH is plotted as the interrupted horizontal line.
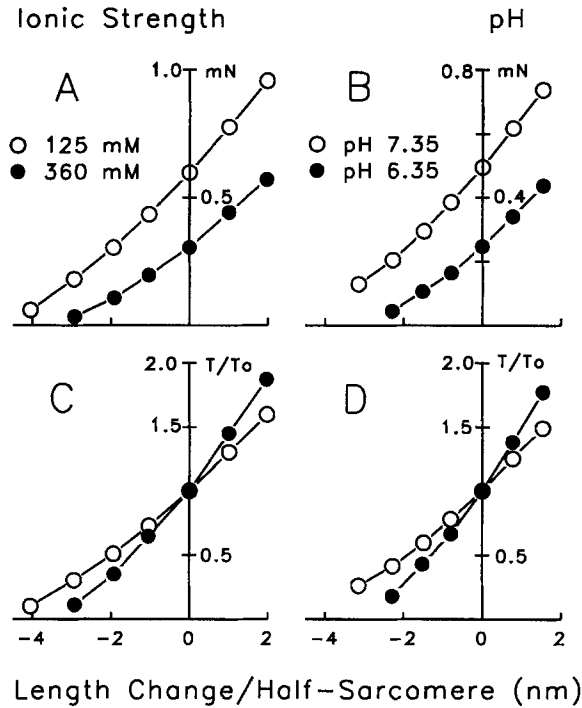
Ionic Strength　　　　　　　　pH

FIGURE 12. T_1 curves indicating relative stiffness at ionic strengths of 125 and 360 mM (A and C) and pH 7.35 and 6.35 (B and D). In the upper panels (A and B) force is plotted in absolute dimensions. In the lower panels (C and D) force is plotted as a fraction of the isometric value. Both the lower pH and the higher ionic strength decrease isometric force by about half and the stiffness by about one-fourth, so that the stiffness/force ratio is increased by about half.

Length Change/Half-Sarcomere (nm)

step size in Fig. 12. As shown, force is decreased nearly twofold by both interventions, while instantaneous stiffness is decreased by only about one-fourth, so that the stiffness/force ratio was increased by half. The curvature of the T_1 curves might have made it difficult to quantify the changes in stiffness exactly, were it not for the fact that the curvature in the two pairs of curves was about the same. This is shown by the values of relative compliance for each step size listed in Table III. The value listed is y_0, the half-sarcomere distance required to bring force to zero if the T_1 curve is linear and passes through the isometric and T_1 points for that step. As shown, the sarcomere value of y_0 is smaller for stretches and small releases than for large releases, but the ratios of the values for the different step sizes under the two conditions does not change much when no extra truncation of the record is expected under one condition. Such extra truncation is expected in the largest fast releases

TABLE III

Relative Sarcomere Compliance $(y_0[nm/P_0])$

Step	Ionic strength (n = 8)			pH (n = 7)		
	125 mM	360 mM	125 mM/360 mM	pH 7.35	pH 6.35	pH 7.35/pH 6.35
1	3.20	2.17	1.50	3.03	1.94	1.56
2	3.16	2.22	1.45	3.02	2.03	1.49
3	3.60	2.85	1.28	3.51	2.33	1.53
4	3.92	2.90	1.38	3.63	2.51	1.46
5	4.09	3.23	1.28	3.87	2.70	1.45

(step 6) at the lower force because force went near or below zero in some of these steps. For this reason, the results obtained from the sixth steps are not listed in Table III. Some extra truncation is also expected with all releases at high ionic strength, where there is rapid relaxation of the extra stiffness.

DISCUSSION

The main conclusion from these experiments is that both high ionic strength and low pH decrease isometric force by detaining crossbridges in low force states. If the sarcomere stiffness is determined mainly by the number of attached crossbridges (Ford, Huxley, and Simmons, 1981), the increased stiffness/force ratio suggests that both interventions decrease force production to a greater extent than they diminish crossbridge attachment. If the individual bridges are attached in either high or low force states on either side of the power-stroke, as proposed by Huxley and Simmons (1971), these results suggest an accumulation of bridges in low force states. Thus, the differences in the transients would be explained if both interventions inhibited some attached crossbridges from passing into the force-producing part of their cycle, and if these low force crossbridges were much more likely to be detached by steps in one direction. If the detachment of the detained bridges in high ionic strength were very fast after release and very slow after stretch, there would be little effect on shortening velocity but a large increase in the stiffness/force ratio, particularly when stiffness is measured with stretches. By comparison, low pH would also cause a large increase in the stiffness/force ratio and the slow detachment of detained bridges during shortening would cause a substantial impediment to shortening and decreased velocities. The excellent agreement between the long-lived extra force change after large releases and the amount of internal load required to diminish maximum velocity further support the conclusion that detained bridges are responsible for the diminished velocity.

The finding that the extra force change reaches a plateau with intermediate size releases raises the question of why this force change does not increase with larger steps. A likely explanation is that when some elastic limit of ~5 nm is exceeded, the detained bridges are forcibly detached, but they quickly reattach at actin sites corresponding to the shorter length, so as to maintain a constant resistance with continued shortening. This explanation is identical to the quantitative model of forced crossbridge detachment and rapid reattachment developed by Brenner (1991) to explain the constant plateau of force seen during sustained lengthening of relaxed muscle.

An important conclusion from these experiments is that all of the observed results can be explained by the proposed effects on the early parts of the attachment phase of the crossbridge cycle. Except for the asymmetrical force changes, the transients scale in exact proportion to the isometric force, suggesting that the later parts of the attachment phase of the cycle are not affected. The additional observation that the resistance imposed by the detained bridges can account quantitatively for the changes in the force–velocity properties seen at low pH further suggests that the remainder of the cycle is not affected. At first sight, this is a somewhat surprising conclusion because all of the transitions in the cycle are probably brought about by the making and breaking of ionic bonds. It might therefore be expected that changes

in pH and ionic strength, which greatly affect protein ionization, would have multiple effects on the cycle. The probable explanation of an absence of more wide ranging effects is that the ionic interactions in the crossbridge cycle are robust, and have evolved to be independent of changes in their environment, at least over the ranges studied here. The absence of pH effects probably results from the hydrogen ion dissociation constants for the responsible protein moieties not being close to those of water (i.e., the pKa's are not near 7). In support of this concept are the findings that the actin binding site on myosin is highly positively charged, while the myosin binding site on actin is very negatively charged (Taylor, 1992). Such strong opposite charges would produce strong binding of the two proteins, and would not be likely to be affected by relatively small pH changes over the neutral range. It is not yet known, however, whether these same sites are responsible for the transitions which we have measured here. A similar mechanism to account for the lack of an effect of ionic strength cannot be specified as precisely, but a possible explanation is that the responsible ionized groups are buried deep in the proteins, and are thus insensitive to the ionic strength of the bathing solutions.
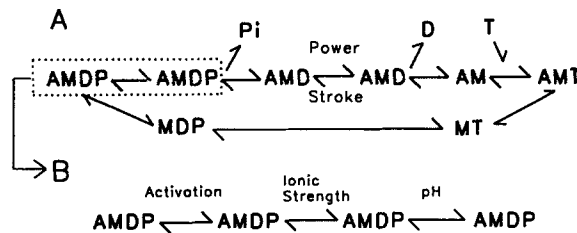

FIGURE 13. Proposed sequence in the crossbridge cycle. The initial part of the attached phase of the cycle enclosed in dashed lines in *A* is expanded to include three transitions in *B*. The first of these is a transition that is inhibited at rest by the activating system. The second transition is inhibited by high ionic strength and the last by low pH.

Specific Proposal

Since Huxley's (1957) proposal that muscle contraction is driven by the cyclical attachment and detachment of crossbridges, work has focused on defining the specific transitions that occur in the cycle. An outcome of this work is the development of schemes such as that in Fig. 13 *A*, designating both the transitions and the order in which they occur. The present discussion is not concerned with the entire scheme, but only with the portion of the cycle enclosed by the dashed lines, indicating that the initial crossbridge attachment occurs in several steps (Fig. 13 *B*). As shown, the bridges move from an initial attached state which can form even in the relaxed muscle to two additional low force states that can form only after activation. We further propose that the two additional states occur in the sequence shown; that is, they move first from the initial attached state to the state in which they are detained by low ionic strength and then to the state in which they are detained by low pH. The reason for making this assignment is the finding that in low pH following release there are small rapid force responses that resemble those seen at high ionic strength. To the extent that these rapid responses result from the same type of

detained bridges under the two conditions, their presence would suggest that they occur in a state that precedes both of the postulated extra transitions. This consideration suggests the order shown in Fig. 13 *B*. To obtain more firm evidence for the proposed scheme, it is necessary to rely on a great deal of previously published work, as follows.

Relationship to Earlier Proposals

Before any discussion of specific proposals, we will define what we mean by a crossbridge state. In this discussion, we envision the crossbridge as undergoing transitions through multiple individual states as it cycles. In some of these transitions, the bridge may undergo a physical movement, such as attachment to actin or a power stroke, while in others a chemical transition may occur on the bridge, such as the hydrolysis of ATP or the release of one of the reaction products. In some cases, the bridge itself may not change, but the change may occur in the environment of the bridge, such as the activation changes in the thin filament that make possible additional crossbridge transitions. The importance of this recognition of different states is that any change in the observed behavior of the bridges indicates a change in state, which must occur by means of a specific pathway.

As first proposed by Huxley (1980), we believe that each of these transitions occurs as a separate stochastic event, so that two or more transitions are not linked together in a single step. The importance of this last point is that it predicts that there will be a specific order to the transitions. When two orders are possible, i.e., when there are branched pathways, more states must be postulated to account for the separate states in each branch. One important consequence of this restriction is that there is a limited number of power strokes, very possibly only one, per cycle, and that bridges exist on either side of this transition in high or low force states. In this construct then, the finding of a decreased force/stiffness ratio, implying a reduced average force per bridge, indicates a shift in the distribution of bridges and not a reduced force in each bridge.

A final caveat about the definitions of crossbridge states has to do with the use of the terms "strong" and "weak" binding states (see Eisenberg and Hill, 1985 for a review of the origins of these terms). It is well known that crossbridges are very tightly bound to thin filaments in the absence of ATP; i.e., the binding constant for these rigor bridges is extremely high. When ATP or another suitable agent is added, the binding constant, as measured in solution, is reduced. Thus, it has become customary to speak in terms of the bridges being in either a strong or a weak binding state. Because the rigor state is believed to be a high force state, the term strong binding is sometimes taken to be synonymous with a force-generating state. The present experiments indicate some difficulty with this terminology. It is obvious that there are more than two or three distinct attached states for a crossbridge, and thus there is likely to be a spectrum of binding constants for the attached bridges, with no simple division into states with high or low binding constants. In addition, it is possible, and even likely, that some of the intermediate low force states have high binding constants, while some high force states have low binding constants. (How else would a bridge detach when it binds ATP at the end of its power stroke?) Thus, the term "strong binding state" does not distinguish a high force state. Perhaps most

importantly, the strength of binding may depend on the direction of strain, as indicated by the comparison of the effects of ionic strength and pH. For all of these reasons, we have not characterized any of the states we can distinguish in terms of the strength of binding.

Relationship to studies of relaxed muscle. In 1968 D. K. Hill described in relaxed muscle a "short range elastic component" that was manifest by a rise in force with small stretches until an elastic limit was reached (Hill, 1968). He interpreted this as being due to crossbridge interactions between the filaments for two reasons: (a) the elastic limit was very short, ~0.2% of muscle length, and equivalent to the expected range of crossbridge function; and (b) the resistance to stretch increased with high osmolality, an intervention that was known to increase heat production, and presumably crossbridge activity, in resting muscle. A similar short-range viscoelasticity in resting muscle was attributed to attached crossbridges in resting muscle by Ford et al. (1977) because it disappeared on stimulation. This short-range stiffness became much more interesting when Brenner, Schoenberg, Chalovich, Greene, and Eisenberg (1982) found that it could be increased to very high levels by lowering the ionic strength in relaxed skinned fibers. This increase in crossbridge attachment could be correlated with the well-known observations that the contractile proteins are more tightly associated at low ionic strengths (Highsmith, 1977). This finding in skinned fibers led to the proposal that the troponin–tropomyosin activating system does not inhibit the initial attachment of cross-bridges to the thin filaments, but instead inhibits the transition of bridges from an initially attached, inactive state to an active state (Brenner et al., 1982).

These studies of relaxed muscle raise the question of whether either of the states in which the bridges are detained by high ionic strength and low pH are the same as the inactive bridges described by Brenner et al. (1982). The most likely conclusion is that they are not, and the reasons for this are different for the two detained states.

The low force bridges detained by high ionic strength in activated muscle differ significantly from those attached by low ionic strength in relaxed muscle in that they are not easily detached by stretch. Another difference between the two types of experiments is that the low force bridges seen here are increased by high ionic strength, whereas the low force bridges seen in the passive muscle are increased by a low ionic strength. Furthermore, Schoenberg (1988) has interpreted his results showing that the greater binding of bridges in relaxed muscle at low ionic strength as being due to a more rapid attachment rather than a decreased detachment. The present experiments suggest that the opposite occurs in activated muscle: that low ionic strength increases the absolute number of attached bridges by decreasing detachment. This decreased detachment occurs because the initially attached bridges are moved to other states where they remain attached to generate force.

The bridges detained at low pH are similar to those seen in the relaxed muscle in that they are readily detached by stretch. Experiments with partial activation suggest, however, that they are not the same state. Since the bridges detained by low pH are manifest mainly in shortening experiments, they would be difficult to recognize in releases of completely relaxed muscle because the whole fiber goes slack when shortened. They could, however, be detected in partially activated fibers because they would resist isotonic shortening. If such bridges were present, there would be an

increasing activation dependence of maximum velocity as pH is lowered. The data in Fig. 3 *B* indicate that the pH effects seen here vary continuously over the physiological range of pH, so that there should be some effect of detained bridges even at neutral pH. After a long period of uncertainty about the effects of activation on velocity (see review by Podolin and Ford, 1983), there has been agreement in several recent studies that there is no dependence of shortening velocity on activation when velocity is measured early in phase 4 of the velocity transients and when activation is varied between 40–50% and 100% of maximum (Moss, 1986; Podolin and Ford, 1986; Ford, Nakagawa, Desper, and Seow, 1991). These finding strongly suggest that the state in which crossbridges are detained by low pH is different from the state in which they attach in the relaxed state.

Since the detained bridges described here appear to be different from those that accumulate in relaxed muscle at low ionic strength, the bridges must undergo at least one transition between their initial attachment and the states in which they are detained by low pH and high ionic strength.

Relationship to energetics. In Huxley's original theory (Huxley, 1957), the crossbridge cycling rate increased progressively with velocity, in the same way that total energy rates appeared to increase in A. V. Hill's original data (Hill, 1938). The increased cycling rate was explained by a shortening of the overall cycle duration at higher velocities, so that both the attachment and detachment rates increased. When Hill (1964) later found that the total energy rate reached a maximum at intermediate velocities, Huxley (1973) was able to explain the new data by proposing that crossbridge attachment occurred in two steps. The first was attachment in a state from which the bridges were not committed to liberating the energy of ATP hydrolysis, and from which they could be detached by shortening without losing energy. When the bridges passed to the second state, they became committed to energy release. In this way, the initial rate of attachment would increase progressively with increased velocity, as postulated by Huxley's original theory (Huxley, 1957), but the maximum energy liberation would occur at intermediate velocities. The present experiments offer direct experimental evidence for one aspect of Huxley's proposal, namely, that bridges are initially attached in a low force state from which they are easily detached by shortening.

Alternative mechanisms. It might seem that it has been tacitly assumed in this discussion that all of the transitions occur in the active part of the crossbridge head. The possibility must also be considered that the interventions in some way alter the part of the crossbridge that makes it compliant. Such unidirectional changes in compliance seem unlikely, but if they were to occur, the foregoing discussion could be made valid by the semantic expedient of including a change in crossbridge spring length under the rubric of a state transition.

A more serious matter is the question of whether the states considered are a part of the normal crossbridge cycle, or whether the interventions cause bridges to accumulate in alternative, paranormal states that are side branches to the normal cycle. We cannot exclude this possibility with certainty, but at least one of the states, that in which the bridges are detained by high ionic strength, appears to have characteristics that are similar to a state postulated to be a part of the normal cycle. The consideration that a portion of the added response produced by low pH resembles

that seen at high ionic strength further suggests that the low pH causes bridges to accumulate in two states that are a part of the cycle.

Correlation with Earlier Studies

Tension transients. The transients described here were very similar to those described earlier for frog skeletal muscle fibers at somewhat colder temperatures (Ford et al., 1977), except that the relative sarcomere stiffness was somewhat greater. The similarities include the presence of four distinct phases, the convex upward shape of the T_2 curve, the amount of sarcomere shortening required to bring the T_2 curve to zero, and the speeding of phase 2 recovery with increasing size of release. These similarities suggest that the contractile mechanism is the same in the two types of muscle. The greater relative stiffness seen in these experiments can be explained by the use of low temperatures in a muscle that is designed to work exclusively at mammalian body temperature. Ford et al. (1977) found that the relative stiffness of frog fibers decreased substantially as the temperature was raised from 0 to 8°C, and this decrease was attributed to an increased average force per bridge. Although we have not measured the effect of temperature in these experiments, it is reasonable to speculate that an increase of a few degrees decrease would bring the relative stiffness to that seen with frog muscle at 0°C. The differences between the muscles would then be explained by the equilibrium constant for the power stroke being slightly higher at a given temperature in frog than rabbit muscle.

Ionic strength effects. It is well known that decreased ionic strength increases isometric force in skinned fibers (Gordon and Godt, 1970; Thames et al., 1974). The earliest studies of the effect of low ionic strength on shortening velocity showed a decrease in maximum velocity, but the authors attributed this decrease to fiber damage produced by the higher forces (Thames et al., 1974). More recent experiments from the same laboratory (Gulati and Podolsky, 1981) indicated that as long as the ionic strength were greater than some minimum value, the damage could be avoided and the maximum velocity appeared to be independent of ionic strength. The present experiments would agree with this more recent conclusion.

There have been several more recent studies confirming the effects of ionic strength on the force velocity curves (e.g., Edman and Mattiazzi, 1981; Julian and Moss, 1981). In addition, Kawai, Wray, and Güth (1990) have concluded from other types of experiments, as we do here, that ionic strength affects only the initial attachment of crossbridges. Finally, while it may be dangerous to extrapolate from solution chemistry to muscle fibers (Geeves, 1991), at least one such solution study has suggested that high ionic strength inhibits an isomerization of the actin-myosin-nucleotide complex that is thought to be a correlate of the force-generating step in intact fibers (Coates, Criddle, and Geeves, 1985).

pH effects. Metzger and Moss (1990) have recently shown that lowered pH decreases maximum velocity, isometric force, and stiffness, with the decrease in force being greater than the decrease in stiffness. The present findings agree, at least qualitatively, with their study, but we have repeated these experiments here for two reasons. The first is so that they can be correlated with changes in the transients measured under identical conditions. The second is that these experiments include one important condition not examined in the earlier experiments: the use of a high

molecular weight polymer to compress the filament lattice to near its normal filament spacing.

It is known that muscle fibers swell when skinned (Godt and Maughan, 1977), and that this swelling is associated with expansion of the filament lattice (Matsubara and Elliot, 1972). Goldman and Simmons (1986) have further shown that uncompressed skinned fibers have highly nonlinear stiffness. Goldman (1987) subsequently showed that this nonlinear stiffness is due to an inability of the crossbridges to withstand negative tension when the lattice is swollen, so that they become more compliant when shortened rapidly. He further showed that as a consequence of the cross-bridges' inability to resist negative forces, uncompressed skinned fibers have much higher maximum velocities than intact fibers or compressed skinned fibers. Thus, maximum velocities measured in the presence and absence of osmotic compression may be determined by two separate processes. In spite of this possibility, the effects of pH were qualitatively similar in the presence and absence of lattice compression.

Conclusions

Since Huxley's proposal (Huxley, 1957) that contraction is generated by the cyclical attachment and detachment of force-generating crossbridges, subsequent studies have shown that there are multiple mechanical and chemical transitions in the cycle. Much of the current work in this area is directed at defining these transitions and determining the sequence in which they occur. Taken together with other work, the present experiments suggest that the attachment of bridges occurs in several steps. Low pH and high ionic strength detain bridges in separate low force states that precede the force-generating power stroke but follow an initial attachment that does not require thin filament activation. The state in which the bridges are detained by high ionic strength resembles a state postulated by Huxley (1973) to account for energetic data. The observation that a part of the force response obtained at low pH resembles that obtained at high ionic strength suggests that the low pH detains bridges in a state following that in which they are detained by high ionic strength.

REFERENCES

Brenner, B. 1983. Technique for stabilizing the striation pattern in maximally calcium-activated skinned rabbit psoas fibers. *Biophysical Journal.* 41:99–102.

Brenner, B. 1991. Rapid dissociation and reassociation of actomyosin cross-bridges during force generation: a newly observed facet of cross-bridge action in muscle. *Proceedings of the National Academy of Sciences, USA.* 88:10490–10494.

Brenner, B., M. Schoenberg, J. M. Chalovich, L. E. Greene, and E. Eisenberg. 1982. Evidence for cross-bridge attachment in relaxed muscle at low ionic strength. *Proceedings of the National Academy of Sciences, USA.* 79:7288–7291.

Chase, P. B., and M. J. Kushmerick. 1988. Effects of pH on contraction of rabbit fast and slow skeletal muscle fibers. *Biophysical Journal.* 53:935–946.

Chiu, Y.-L., S. Karwash, and L. E. Ford. 1978. A piezoelectric force transducer for single muscle cells. *American Journal of Physiology.* 253:C143–C146.

Chiu, Y.-C., J. Quinlan, and L. E. Ford. 1985. A system for automatic activation of skinned muscle fibers. *American Journal of Physiology.* 249:C522–C526.

Coates, J. H., A. H. Criddle, and M. A. Geeves. 1985. Pressure relaxation of pyrene-labelled actin and myosin subfragment 1 from rabbit skeletal muscle. *Biochemical Journal.* 232:351–356.

Cooke, R., K. Franks, G. B. Luciani, and E. Pate. 1988. The inhibition of rabbit skeletal muscle contraction by hydrogen ions and phosphate. *Journal of Physiology.* 395:77–97.

Edman, K. A. P., and A. P. Mattiazzi. 1981. Effects of fatigue and altered pH on isometric force and velocity of shortening at zero load in frog muscle fibres. *Journal of Muscle Research and Cell Motility.* 2:321–334.

Eisenberg, E., and T. L. Hill. 1985. Muscle contraction and free energy transduction in biological systems. *Science.* 227:999–1006.

Fenster, S. D., and L. E. Ford. 1985. SALT: a threaded interpretive language interfaced to BASIC for laboratory applications. *Byte.* 10(6):147–164.

Ford, L. E. 1991. Mechanical manifestations of activation in cardiac muscle. *Circulation Research.* 68:621–637.

Ford, L. E., and R. Forman. 1974. Tetanized cardiac muscle. *Ciba Foundation Symposia.* 24:137–150.

Ford, L. E., A. F. Huxley, and R. M. Simmons. 1977. Tension responses to sudden length changes in stimulated frog muscle fibres near slack length. *Journal of Physiology.* 269:441–515.

Ford, L. E., A. F. Huxley, and R. M. Simmons. 1981. The relation between stiffness and filament overlap in stimulated frog muscle fibres. *Journal of Physiology.* 311:219–249.

Ford, L. E., K. Nakagawa, J. Desper, and C. Y. Seow. 1991. Effect of osmotic compression on the force-velocity properties of glycerinated rabbit skeletal muscle cells. *Journal of General Physiology.* 97:73–88.

Geeves, M. A. 1991. The dynamics of actin and myosin association and the crossbridge model of muscle contraction. *Biochemical Journal.* 274:1–14.

Godt, R. E., and D. W. Maughan. 1977. Swelling of skinned muscle fibers of the frog. *Biophysical Journal.* 19:103–116.

Goldman, Y. E. 1987. Measurement of sarcomere shortening in skinned fibers from frog muscle by white light diffraction. *Biophysical Journal.* 52:57–68.

Goldman, Y. E., and R. M. Simmons. 1984. Control of sarcomere length in skinned muscle fibres of *Rana temporaria* during mechanical transients. *Journal of Physiology.* 350:497–518.

Goldman, Y. E., and R. M. Simmons. 1986. The stiffness of frog skin muscle fibres at altered lateral filament spacing. *Journal of Physiology.* 378:175–194.

Gordon, A. M., and R. E. Godt. 1970. Some effects of hypertonic solutions on contraction and excitation-contraction coupling in frog skeletal muscle. *Journal of General Physiology.* 55:254–275.

Gulati, J., and R. J. Podolsky. 1981. Isotonic contraction of skinned muscle fibers on a slow time base. *Journal of General Physiology.* 78:233–257.

Highsmith, S. 1977. The effects of temperature and salts on myosin subfragment-1 and f-actin association. *Archives of Biochemistry and Biophysics.* 180:404–408.

Hill, A. V. 1938. The heat of shortening and the dynamic constants of muscle. *Proceedings of the Royal Society of London, Series B.* 126:136–195.

Hill, A. V. 1964. The effect of load on the heat of shortening of muscle. *Proceedings of the Royal Society of London, Series B.* 159:297–318.

Hill, D. K. 1968. Tension due to interaction between the sliding filaments in resting striated muscle: the effect of stimulation. *Journal of Physiology.* 199:637–684.

Huxley, A. F. 1957. Muscle structure and theories of contraction. *Progress in Biophysics and Biophysical Chemistry.* 7:255–318.

Huxley, A. F. 1973. A note suggesting that the cross-bridge attachment during muscle contraction may take place in two stages. *Proceedings of the Royal Society of London, Series B.* 183:83–86.

Huxley, A. F. 1980. Reflections on Muscle. Princeton University Press, Princeton, NJ. 111 pp.

Huxley, A. F., and R. M. Simmons. 1971. Proposed mechanism of force generation in striated muscle. *Nature.* 233:533–538.

Huxley, A. F., and R. M. Simmons. 1972. Mechanical transients and the origin of muscular force. *Cold Spring Harbor Symposia on Quantitative Biology.* 37:669–680.

Julian, F. J., and R. L. Moss. 1981. Effects of calcium and ionic strength on shortening velocity and tension development in frog skinned muscle fibres. *Journal of Physiology.* 311:170–199.

Kawai, M., J. S. Wray, and K. Güth. 1990. Effect of ionic strength on crossbridge kinetics as studied by sinusoidal analysis, ATP hydrolysis rate and x-ray diffraction techniques in chemically skinned rabbit psoas fibres. *Journal of Muscle Research and Cell Motility.* 11:392–402.

Matsubara, I., and G. F. Elliot. 1972. X-ray diffraction studies on skinned single fibres of frog skeletal muscle. *Journal of Molecular Biology.* 72:657–669.

Metzger, J. M., and R. L. Moss. 1987. Greater hydrogen ion-induced depression of tension and velocity in skinned fibres of rat fast than slow muscles. *Journal of Physiology.* 393:727–742.

Metzger, J. M., and R. L. Moss. 1990. Effects on tension and stiffness due to reduced pH in mammalian fast- and slow-twitch skinned skeletal muscle fibres. *Journal of Physiology.* 428:737–750.

Moss, R. L. 1986. Effects on shortening velocity of rabbit skeletal muscle due to variations in the level of thin-filament activation. *Journal of Physiology.* 377:487–505.

Podolin, R. A., and L. E. Ford. 1983. The influence of calcium on shortening velocity of skinned frog muscle cells. *Journal of Muscle Research and Cell Motility.* 4:263–282.

Podolin, R. A., and L. E. Ford. 1986. Influence of partial activation on force-velocity properties of frog skinned muscle fibers in millimolar magnesium ion. *Journal of General Physiology.* 87:607–631.

Schoenberg, M. 1988. Characterization of the myosine adenosine triphosphate (M·ATP) crossbridge in rabbit and frog skeletal muscle fibers. *Biophysical Journal.* 54:135–148.

Seow, C. Y., and L. E. Ford. 1991. Shortening velocity and power output of skinned muscle fibers from mammals having a 25,000-fold range of body size. *Journal of General Physiology.* 97:541–560.

Seow, C. Y., and L. E. Ford. 1992. Contribution of damped passive recoil to the measured shortening velocity of skinned rabbit and sheep muscle fibres. *Journal of Muscle Research and Cell Motility.* 13:295–307.

Sweeney, H. L., S. A. Corteselli, and M. J. Kushmerick. 1987. Measurements on permeabilized skeletal muscle fibers during continuous activation. *American Journal of Physiology.* 252:C575–C580.

Taylor, E. W. 1992. Mechanism and energetics of actomyosin ATPase. *In* The Heart and Cardiovascular System. 2nd ed. H. A. Fozzard, editor. Raven Press, Ltd., New York. 1281–1293.

Thames, M. D., L. E. Teichholz, and R. J. Podolsky. 1974. Ionic strength and the contraction kinetics of skinned muscle fibres. *Journal of General Physiology.* 63:509–530.

Wirth, P., and L. E. Ford. 1986. Five laboratory interfacing packages. *Byte.* 11(7):303–312.